Measurement of Zeeman Shift of Cesium Atoms Using an Optical Nanofiber *

Chuan-Biao Zhang(张传标)[1,2], Dian-Qiang Su(苏殿强)[1,2], Zhong-Hua Ji(姬中华)[1,2], Yan-Ting Zhao(赵延霆)[1,2**], Lian-Tuan Xiao(肖连团)[1,2], Suo-Tang Jia(贾锁堂)[1,2]

[1]*State Key Laboratory of Quantum Optics and Quantum Optics Devices, Institute of Laser Spectroscopy, Shanxi University, Taiyuan 030006*

[2]*Collaborative Innovation Center of Extreme Optics, Shanxi University, Taiyuan 030006*

(Received 17 May 2018)

Nanofibers have many promising applications because of their advantages of high power density and ultralow saturated light intensity. We present here a Zeeman shift of the Doppler-broadened cesium D_2 transition using a tapered optical nanofiber in the presence of a magnetic field. When a weak magnetic field is parallel to the propagating light in the nanofiber, the Zeeman shift rates for different circularly polarized spectra are observed. For the σ^+ component, the typical linear Zeeman shift rates of $F = 3$ and $F = 4$ ground-state cesium atoms are measured to be 3.10(±0.19) MHz/G and 3.91(±0.16) MHz/G. For the σ^- component, the values are measured to be −2.81(±0.25) MHz/G, and −0.78(±0.28) MHz/G. The Zeeman shift using the tapered nanofiber can help to develop magnetometers to measure the magnetic field at the narrow local region and the dispersive signal to lock laser frequency.

PACS: 32.60.+i, 32.10.Fn, 81.07.−b DOI: 10.1088/0256-307X/35/8/083201

Nanofiber systems[1] have gradually become popular and promising in a great number of applications, such as in highly efficient optical coupling devices,[2] spectroscopy,[3] quantum memory stations,[4] and optical manipulation.[5] Due to their strong confinement of the electromagnetic field, low-power nonlinearities[6] become possible through compression of the optical mode area which can interact with the atoms. Optical nanofiber systems have also recently been used to demonstrate nanowatt-level saturated absorption,[7] electromagnetically induced transparency,[8] two-photon absorption,[9] and all-optical modulation.[10] In addition, nanofibers can be directly coupled by a tapered transition to a standard optical fiber due to their flexibility, which may be connected directly to fiber networks. Tiny volume and ultrahigh power density also provide much convenience for studying the interaction between light and atoms.

Cesium atoms are extensively used in frequency standard,[11] communication,[12] and space applications.[13] Consequently, it is important to further study the properties of cesium atoms. The traditional Zeeman frequency shift is studied in the atomic cell, which can achieve stabilization of laser frequency.[14] In addition, precise measurement of pulsed magnetic fields[15] and coherent manipulation of neutral atoms[16] can also be achieved using the Zeeman shift. Compared with the atomic cell, nanofibers have the advantages of narrow region and high power density, and they are suitably used for studying the nonlinear effect of weak light. Amy *et al.* measured the Zeeman shift of rubidium atoms in a nanofiber,[17] and we here introduce a nanofiber system to measure the Zeeman shift of the cesium atom based on its tiny volume, and strong confinement of the electromagnetic field. This method just needs an incident beam with ultralow power (order of nW), which is a remarkable advantage compared with the traditional Zeeman shift in cell. The nanofiber is successfully fabricated by the flame-brush technology and it is put into a vacuum chamber. The temperature of the chamber and optical nanofiber is controlled to warrant the appropriate atomic density and against accumulation of atoms on the nanofiber surface. In the absence of an external magnetic field, atomic energy levels are degenerate. However, their degeneracy is broken and atomic magnetic sublevels will split with the weak homogeneous magnetic field produced by a pair of Helmholtz coils. As a result, we observe the Zeeman shift of two circularly polarized spectra after exerting an external magnetic field on the waist of the nanofiber in cesium vapor.

In our experiment, the optical nanofiber is fabricated from an 852 nm single mode optical fiber by the flame-brush technology.[18] During the process of pulling, the nanofiber volume keeps constant and the optical fiber ultimately has an extremely small diameter. The nanofiber diameter is measured to be 507 nm by a scanning electron microscope[19] and its length is about 5 mm. The transmission ratio of the tapered nanofiber monitored is up to 98%[20] in the end. We put it into the vacuum chamber by employing a standard Teflon fiber feed-through[21,22] system. Heating

*Supported by National Key Research and Development Program of China under Grant No 2017YFA0304203, the National Natural Science Foundation of China under Grant Nos 61675120 and 11434007, the National Natural Science Foundation of China for Excellent Research Team under Grant No 61121064, the Shanxi Scholarship Council of China, the 1331KSC, the PCSIRT under Grant No IRT13076, and the Applied Basic Research Project of Shanxi Province under Grant No 201601D202008.

**Corresponding author. Email: zhaoyt@sxu.edu.cn

installation[23] is designed to heat the nanofiber gradually up to 90℃, which is higher than the chamber temperature (about 80℃) against accumulation of cesium atoms.

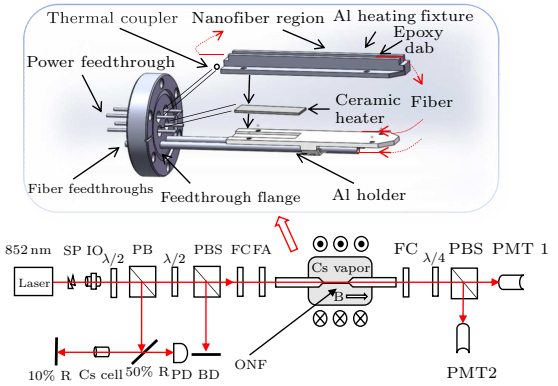

Fig. 1. (Color online) Schematic of experimental setup. SP: shaping prism, IO: optical isolator, $\lambda/2$: half-wave plate, PBS: polarizing beam splitter, FC: fiber coupler, FA: fiber attenuator, 10% R: 10% reflector, 50% R: 50% reflector, PD: photodetector, BD: beam dump, ONF: optical nanofiber, $\lambda/4$: quarter-wave plate, and PMT: photomultiplier tube. The upper picture is the heating system of the nanofiber composed of flange, feedthrough, Al heating fixture, Al holder, and ceramic heater.

A schematic diagram of the experimental setup is shown in Fig. 1. The incident beam from the 852 nm diode laser passes through a shaping prism and an optical isolator. When the input beam arrives at the polarizing beam splitter, it is separated into two parts. The reflected beam is used to build the saturated absorption spectroscopy, and the transmitted beam is launched into the $\lambda/2$ plate and the polarizing beam splitter for the purpose of adjusting the beam intensity further. Then the beam enters the fiber attenuator, which can reduce the beam power further to the order of nanowatt, and it is coupled into the optical nanofiber by a fiber coupler. The output beam from the other end of the fiber is detected by two photomultiplier tubes after it passes the fiber coupler, the $\lambda/4$ plate, and the polarizing beam splitter. The centers of the Helmholtz coils are aligned with the waist of the nanofiber, which locates in the homogeneous magnetic field region. The heating equipment of the nanofiber is shown in the inset of Fig. 1, and the fiber is mounted on two higher ends with UV epoxy of a piece of aluminum heating fixture. The aluminum heating fixture sits on a ceramic heater and is held (with set screws) on an aluminum holder. The aluminum holder is mounted on the feed-through flange used for feeding the fiber in and out of the flange. Power feedthrough is designed for the ceramic heater and thermal couple. The thermal couple is placed on the aluminum heating fixture to monitor the real-time temperature of the nanofiber.

As described above, a pair of Helmholtz coils are used to produce a homogeneous magnetic field. The magnetic field at the center of two coils is given by

$$B = \frac{8}{5^{3/2}} \sum_{1}^{N} \frac{1}{R_{\rm i}} \mu_0 N I,$$

where μ_0 is the permeability of a vacuum, N is the turns of coils, I is the applied current of coils, and $R_{\rm i}$ is the radius of the ith coil. In our experiment, we made 200 turns coils with diameters in the range of 10–13 cm to produce a magnetic field with 0–100 Gauss. We can obtain the relationship between magnetic field and current at the central axis of two coils and the results are shown in Fig. 2.

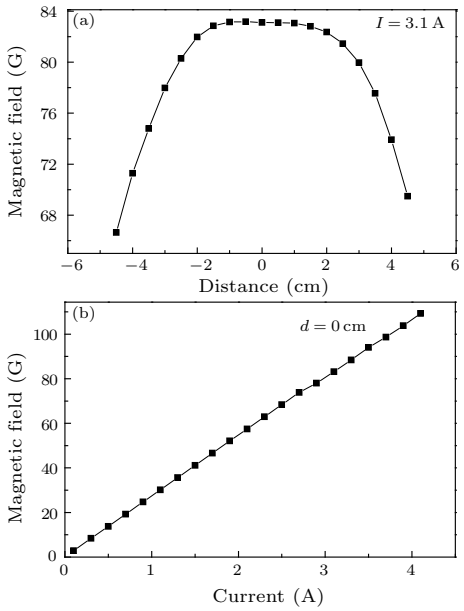

Fig. 2. (Color online) External magnetic field as a function of distance along the center of two coils (a) and applied current (b).

We can obtain that there is a homogeneous distribution of magnetic field between a pair of Helmholtz coils with a length of about 4 cm, the magnetic field changes uniformly with current at the center of two electrified coils, and the increasing rate of the magnetic field is 26.58(±0.11) G/A.

The linear polarization in the optical nanofiber can be considered as the coherent superposition of two orthogonal circular polarization states, σ^+ and σ^- polarization light of equal intensities. In the absence of a magnetic field, the two atomic transitions are degenerate and absorb both polarizations equally. If a magnetic field exists, this degeneracy will be lifted (the Zeeman shift) and the system will become dichroic. The σ^+ and σ^- spectra will be absorbed at the higher and lower frequencies, respectively. We can obtain the frequency shift according to[24]

$$\delta\omega = g_{\rm F} \frac{\mu_{\rm B} B}{\hbar} m_{\rm F},$$

where $g_{\rm F}$ is the Landé g-factor, $\mu_{\rm B}$ is the Bohr magneton, B is the applied magnetic field, and $m_{\rm F}$ is the magnetic quantum number.

The saturated absorption spectroscopy of the transition of the cesium D_2 line as a frequency reference signal is obtained by a photodetector and can be seen in a four-channel digital signal oscilloscope, as shown in the blue lines in Fig. 3. We turn on the current of the cesium dispenser, and cesium atoms will distribute over the entire chamber several minutes later. Atoms will interact with an evanescent field on the waist of the nanofiber[25] and we can observe the absorption spectroscopy of the cesium D_2 line. The laser frequency is detuned from $6^2S_{1/2}, F = 3 \rightarrow 6^2P_{3/2}, F' = 3$ (Fig. 3(a)) and from $6^2S_{1/2}, F = 4 \rightarrow 6^2P_{3/2}, F' = 5$ transitions (Fig. 3(b)), respectively. In the absence of the external magnetic field, and the circularly polarized absorption spectrum through the nanofiber is recorded on a digital oscilloscope (shown with red solid lines). Applying an external magnetic field (58 G) on the waist of the nanofiber, we can clearly observe a frequency shift of the σ^+ component and the σ^- component at the higher frequency and lower frequency (shown with red dashed lines), respectively.

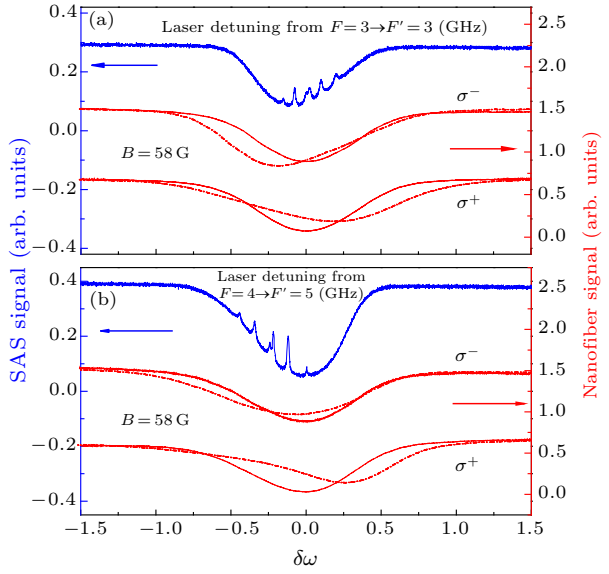

Fig. 3. (Color online) Absorption spectrum of σ^+ and σ^- circularly polarized spectra in the absence (red solid line) and presence of the magnetic field (58 G) (red dashed line) from ground states $F = 3$ (a) and $F = 4$ (b). The saturated absorption spectroscopy (blue line) acts as the reference frequency.

Zeeman spitting as a function of magnetic field is demonstrated in Fig. 4. Frequency shifts of σ^+ and σ^- circularly polarized spectra are increasing and decreasing with the increasing magnetic field, respectively. When the external magnetic field is zero, the energy level will not spit and in the presence of an external magnetic field, there exist different frequency shifts for different ground states. We can obtain that σ^+ and σ^- circularly polarized spectra are asymmetric. The reasons for unharmonious spitting are multiple, such as individual Landé g-factors for each transition while optical pumping[26,27] needs to be considered to remove this inconsistency. In the nanofiber system, a detailed analysis of all fiber-related birefringence effects[28] is required. Also, specifically to a nanofiber, there may be effects from the atom-surface interactions at the fiber waist. During the measurements presented here, the intensities of the two spectra have a tendency to vary in magnitude as a function of time. To maintain the signal, it is necessary to rotate the $\lambda/2$ plate by a few degrees. In addition, we propose that the change of beam polarization in the nanofiber resulting from fiber birefringence needs to be addressed by implementing either a Berek compensator[29] before the fiber coupler or a polarization-maintaining tapered fiber.[30] As shown in Fig. 4, the frequency shift will increase and decrease the σ^+ component and the σ^- component, respectively, for both the $F = 3 \rightarrow F'$ transition and the $F = 4 \rightarrow F'$ transition, and those data are obtained by an average of 16 times in steps of 0.2 A. As a result, the typical frequency shift rates of $F = 3$ and $F = 4$ ground states are measured. For the σ^+ component, the shift rates of $F = 3$ and $F = 4$ ground-state cesium atoms are measured to be $3.10(\pm0.19)$ MHz/G and $3.91(\pm0.16)$ MHz/G. For the σ^- component, the values are measured to be $-2.81(\pm0.25)$ MHz/G and $-0.78(\pm0.28)$ MHz/G. Compared with the Zeeman shift rates[31] in the cesium cell, the measured results of Zeeman shift rates of the cesium D_2 line in the nanofiber system are at the same order of magnitude. However, we successfully achieve measurement of Zeeman shift of cesium D_2 line rates at ultralow power (nanowatt level).

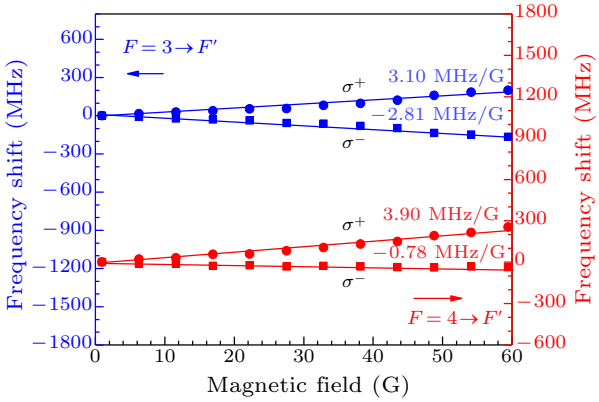

Fig. 4. (Color online) Zeeman shift of σ^+ and σ^- circularly polarized spectra from $F = 3$ (blue) and $F = 4$ (red) ground states.

In summary, we have successfully observed the Zeeman shift phenomenon of the cesium D_2 line using an optical nanofiber and measured the Zeeman shift rates. An optical nanofiber heating installation is designed to guarantee ultrahigh transmission of the nanofiber. A pair of Helmholtz coils are used to produce a homogeneous magnetic field in definite distance at different currents. When a dc magnetic field has the same propagation direction with incident light, the σ^+ and σ^- spectra are absorbed at the higher and lower frequencies, respectively. For the σ^+ compo-

nent, the shift rates of $F = 3$ and $F = 4$ ground-state cesium atoms are measured to be $3.10(\pm 0.19)$ MHz/G and $3.91(\pm 0.16)$ MHz/G. For the σ^- component, the values are measured to be $-2.81(\pm 0.25)$ MHz/G and $-0.78(\pm 0.28)$ MHz/G. Based on the nanofiber system, we intend to stabilize the frequency of the laser by a dichroic atomic-vapor laser lock (DAVLL), which depends on the difference in absorption rates of the two components. In addition to the advantages of the DAVLL technique,[32] such as the large recapture range and free modulation, this nanofiber system can provide a stable frequency reference due to the low variety of magnetic field in a local narrow region.

References

[1] Wang X Z, Li Y and Bao X Y 2009 *Appl. Opt.* **48** 6827
[2] Fenton E F, Khan A, Solano P, Orozco L A and Fredrik K F 2018 *Opt. Lett.* **43** 1534
[3] Cao Y C, Jin W, Ho L H and Liu Z B 2012 *Opt. Lett.* **37** 214
[4] Gouraud B, Maxein D, Nicolas A, Morin O and Laurat J 2015 *Phys. Rev. Lett.* **114** 180503
[5] Li Y and Hu Y J 2013 *Chin. Phys.* B **22** 34206
[6] Spillane S M, Pati G S, Salit K, Hall M, Kumar P, Beausoleil R G and Shahriar M S 2008 *Phys. Rev. Lett.* **100** 233602
[7] Thapa R, Knabe K, Faheem M, Naweed A, Weaver O L and Corwin K L 2006 *Opt. Lett.* **31** 2489
[8] Jones D E, Franson J D and Pittman T B 2015 *Phys. Rev.* A **92** 043806
[9] Hendrickson S M, Lai M M, Pittman T B and Franson J D 2010 *Phys. Rev. Lett.* **105** 173602
[10] Salit K, Salit M, Krishnamurthy S, Wang Y, Kumar P and Shahriar M S 2011 *Opt. Express* **19** 22874
[11] Bize S, Laurent P, Abgrall M, Marion H et al 2005 *J. Phys.* B **38** S449
[12] Balykin V I, Hakuta K, Le K F, Liang J Q and Morinaga M 2004 *Phys. Rev.* A **70** 011401
[13] Laurent P, Abgrall M, Jentsch C, Lemonde P, Santarelli G, Clairon A, Maksimovic I et al 2006 *Appl. Phys.* B **84** 683
[14] Beverini N, Maccioni E, Marsili P, Ruffini A and Sorrentino F 2001 *Appl. Phys.* B **73** 133
[15] King P W and Learner R C M 1971 *Proc. R. Soc. London Ser.* A **323** 431
[16] Treutlein P, Hommelhoff P, Steinmetz T, Hänsch T W and Reichel J 2004 *Phys. Rev. Lett.* **92** 203005
[17] Watkins A, Tiwari V B, Jonathan M, Ward J M, Deasy K and Chormaic S N 2013 *Proc. SPIE* **8785** 87850S
[18] Sorensen H L, Polzik E S and Appel J 2014 *J. Lightwave Technol.* **32** 1886
[19] Wiedemann U, Karapetyan K, Dan C, Pritzkau D, Alt W, Irsen S and Meschede D 2010 *Opt. Express* **18** 7693
[20] Hoffman J E, Ravets S, Grover J A, Solano P, Kordell P R, Wong J D, Orozco L A and Rolston S L 2014 *AIP Adv.* **4** 067124
[21] Morrissey M J, Deasy K, Wu Y Q, Chakrabarti S and Chormaic S N 2009 *Rev. Sci. Instrum.* **80** 053102
[22] Davidson I A, Azzouz H, Hueck K and Bourennane M 2016 *Rev. Sci. Instrum.* **87** 053104
[23] Lai M M, Franson J D and Pittman T B 2013 *Appl. Opt.* **52** 2595
[24] Gunawardena M, Hess P W, Strait J and Majumder P K 2008 *Rev. Sci. Instrum.* **79** 103110
[25] Vetsch E, Reitz D, Sagué G, Schmidt R, Dawkins S T and Rauschenbeutel A 2010 *Phys. Rev. Lett.* **104** 203603
[26] Smith D A and Hughes I G 2004 *Am. J. Phys.* **72** 631
[27] Lindvall T and Tittonen I 2009 *Phys. Rev.* A **80** 032505
[28] Lobov G S, Marinins A, Etcheverry S, Zhao Y C, Vasileva E, Sugunan A, Laurell F, Thylén L, Wosinski L, Östling M, Toprak M S and Popov S 2017 *Opt. Mater. Express* **7** 52
[29] Dawkins S T, Mitsch R, Reitz D, Vetsch E and Rauschenbeutel A 2011 *Phys. Rev. Lett.* **107** 243601
[30] Jung Y M, Brambilla G and Richardson D J 2010 *Opt. Lett.* **35** 2034
[31] Takeshi I, Shinichi O and Motoichi O 1989 *Jpn. J. Appl. Phys.* **28** L1839
[32] Corwin K L, Lu Z T, H, C F, Epstein R J and Wieman C E 1998 *Appl. Opt.* **37** 3295